

# The Effects of the Novel, Reversible Epidermal Growth Factor Receptor/ErbB-2 Tyrosine Kinase Inhibitor, GW2016, on the Growth of Human Normal and Tumor-derived Cell Lines *in Vitro* and *in Vivo*

David W. Rusnak,<sup>1</sup> Karen Lackey, Karen Affleck, Edgar R. Wood, Krystal J. Alligood, Nelson Rhodes, Barry R. Keith, Doris M. Murray, Kimberly Glennon, W. Blaine Knight, Robert J. Mullin, and Tona M. Gilmer

Departments of Cancer Biology [D. W. R., K. J. A., N. R., B. R. K., D. M. M., R. J. M., T. M. G.], Receptor Biochemistry [E. R. W., W. B. K.], and Medicinal Chemistry [K. L., K. G.], GlaxoSmithKline, Research Triangle Park, North Carolina 27709, and Department of Respiratory Systems, GlaxoSmithKline, Stevenage, Hertfordshire SG1 2NY, United Kingdom [K. A.]

## Abstract

The epidermal growth factor receptor (EGFR) and ErbB-2 transmembrane tyrosine kinases are currently being targeted by various mechanisms in the treatment of cancer. GW2016 is a potent inhibitor of the ErbB-2 and EGFR tyrosine kinase domains with  $IC_{50}$  values against purified EGFR and ErbB-2 of 10.2 and 9.8 nM, respectively. This report describes the efficacy in cell growth assays of GW2016 on human tumor cell lines overexpressing either EGFR or ErbB-2: HN5 (head and neck), A-431 (vulva), BT474 (breast), CaLu-3 (lung), and N87 (gastric). Normal human foreskin fibroblasts, nontumorigenic epithelial cells (HB4a), and nonoverexpressing tumor cells (MCF-7 and T47D) were tested as negative controls. After 3 days of compound exposure, average  $IC_{50}$  values for growth inhibition in the EGFR- and ErbB-2-overexpressing tumor cell lines were  $<0.16 \mu\text{M}$ . The average selectivity for the tumor cells versus the human foreskin fibroblast cell line was 100-fold. Inhibition of EGFR and ErbB-2 receptor autophosphorylation and phosphorylation of the downstream modulator, AKT, was verified by Western blot analysis in the BT474 and HN5 cell lines. As a measure of cytotoxicity versus growth arrest, the HN5 and BT474 cells were assessed in an outgrowth assay after a transient exposure to GW2016. The cells were treated for 3 days in five concentrations of GW2016, and cell growth was monitored for an additional 12 days after removal of the compound. In each of these tumor cell lines, concentrations of GW2016 were reached where

outgrowth did not occur. Furthermore, growth arrest and cell death were observed in parallel experiments, as determined by bromodeoxyuridine incorporation and propidium iodide staining. GW2016 treatment inhibited tumor xenograft growth of the HN5 and BT474 cells in a dose-responsive manner at 30 and 100 mg/kg orally, twice daily, with complete inhibition of tumor growth at the higher dose. Together, these results indicate that GW2016 achieves excellent potency on tumor cells with selectivity for tumor versus normal cells and suggest that GW2016 has value as a therapy for patients with tumors overexpressing either EGFR or ErbB-2.

## Introduction

The EGFR<sup>2</sup> and ErbB-2 are members of the type I receptor tyrosine kinase family and have been investigated as potential targets for cancer therapy because of their overexpression in a variety of neoplastic tissues (1). With the exception of ErbB-3, which acts as a noncatalytic partner to other erbB family members, the type I receptors have functional tyrosine kinase catalytic domains. When ligand binds to type I receptors, dimerization occurs. This causes a conformational change in the receptor that activates the kinase domain and results in autophosphorylation and initiation of divergent signal transduction cascades (2). Whereas ErbB-2 is generally thought to be orphaned from a high-affinity ligand, it participates in signaling by heterodimerization with ligand-bound members of the type I receptor family. EGFR and ErbB-2 are known to signal through the Ras pathway, stimulating cell division (3), and through the PI3K pathway, resulting in cell growth and survival (1). Because these effects on cell growth and survival are dependent on the catalytic activity of EGFR and ErbB-2, it is believed that inhibition of this activity could provide a therapeutic opportunity for patients with tumors expressing elevated levels of EGFR and ErbB-2.

Recent efforts to design small molecule inhibitors of EGFR have generated encouraging preclinical and clinical results (2–8). We have reported previously the discovery of a number of small molecule, dual EGFR/ErbB-2, tyrosine kinase inhibitors with activity in preclinical tumor models (9, 10). This study describes the activity of a novel small molecule, GW2016, on normal and tumor-derived human cells in cul-

Received 8/27/01; revised 10/17/01; accepted 10/24/01.

The costs of publication of this article were defrayed in part by the payment of page charges. This article must therefore be hereby marked *advertisement* in accordance with 18 U.S.C. Section 1734 solely to indicate this fact.

<sup>1</sup> To whom requests for reprints should be addressed, at Department of Cancer Biology, GlaxoSmithKline, 5 Moore Drive, Research Triangle Park, NC 27709.

<sup>2</sup> The abbreviations used are: EGFR, epidermal growth factor receptor; PI3K, phosphatidylinositol 3'-kinase; HTRF, homogenous time resolved fluorescence; MEK, mitogen-activated protein/extracellular signal-regulated kinase kinase; HFF, human foreskin fibroblast; RIPA, radioimmunoprecipitation assay; v/v, volume for volume; w/v, weight for volume; TBST, Tris-buffered saline plus Tween 20; FBS, fetal bovine serum; BrdUrd, bromodeoxyuridine.

ture and in human tumor xenograft models. GW2016 is a potent inhibitor of EGFR and ErbB-2 tyrosine kinase catalytic activity and is selective for EGFR and ErbB-2 *versus* other proliferative kinases. Treatment of cell lines with GW2016 results in potent inhibition of tumor cell growth, increased tumor cell death, and selectivity for growth inhibition of tumor cell lines *versus* normal cells.

## Materials and Methods

**Synthesis.** GW2016, *N*-{3-Chloro-4-[(3-fluorobenzyl)oxy]phenyl}-6-[5-({[2-(methylsulfonyl)ethyl]amino}methyl)-2-furyl]-4-quinazolinamine, was synthesized as described (11). OSI-774, [6,7-bis(2-methoxy-ethoxy)quinazoline-4-yl]-(3-ethynylphenyl)amine, was synthesized as described (12). ZD1839, 4-(3-chloro-4-fluoro-anilino)-7-methoxy-6-(3-morpholinopropoxy) quinazoline, was synthesized as described (13).

**In Vitro Kinase Assays.** The intracellular kinase domains of EGFR, ErbB-2, and ErbB4 were purified from a baculovirus expression system. EGFR, ErbB-2, and ErbB-4 reactions were performed in 96-well polystyrene round-bottomed plates in a final volume of 45  $\mu$ l. Reaction mixtures contained 50 mM 4-morpholinepropanesulfonic acid (pH 7.5), 2 mM  $MnCl_2$ , 10  $\mu$ M ATP, 1  $\mu$ Ci of [ $\gamma$ - $^{33}P$ ] ATP/reaction, 50  $\mu$ M Peptide A [Biotin-(amino hexanoic acid)-EEEEYFELVAKK-CONH<sub>2</sub>; Quality Controlled Biochemicals, Inc.], 1 mM dithiothreitol, and 1  $\mu$ l of DMSO containing serial dilutions of GW2016 beginning at 10  $\mu$ M. The reaction was initiated by adding the indicated purified type-1 receptor intracellular domain. The amount of enzyme added was 1 pmol/reaction (20 nM). Reactions were terminated after 10 min at 23°C by adding 45  $\mu$ l of 0.5% phosphoric acid in water. The terminated reaction mix (75  $\mu$ l) was transferred to phosphocellulose filter plates (Millipore, Marlborough, MA). The plates were filtered and washed three times with 200  $\mu$ l of 0.5% phosphoric acid. Scintillation cocktail (50  $\mu$ l, Optiphase; Wallac) was added to each well, and the assay was quantified by counting in a Packard Topcount. (Packard Instrument Co.).

The catalytic domains of vascular endothelial growth factor receptor 2, c-Fms, c-Src, CDK1, CDK2, and Tie-2 were expressed and purified using the baculovirus expression system. Kinase assays were performed as described above with the following modifications. c-Fms assays contained: 10 nM enzyme, 50 mM 4-morpholinepropanesulfonic acid (pH 7.5), 10 mM  $MgCl_2$ , 20  $\mu$ M ATP, and 200  $\mu$ M Peptide A. The reaction was allowed to proceed for 30 min, terminated, and quantified as described above. Vascular endothelial growth factor receptor 2 assays contained: 10 nM enzyme, 100 mM HEPES (pH 7.5), 0.1 mg/ml BSA fraction V (Sigma Chemical Co., St. Louis, MO), 0.1 mM DTT, 360 nM peptide A, 75  $\mu$ M ATP, and 5 mM  $MgCl_2$ . The reaction was allowed to proceed for 40 min. Product was detected using an HTRF procedure (14). Briefly, the reactions were quenched by adding 100  $\mu$ l of 100 mM HEPES (pH 7.5), 100 mM EDTA, 45 nM streptavidin linked-allophycocyanin (Molecular Probes), and 3 nM europium-conjugated antiphosphotyrosine antibody (Wallac). Product was detected using a Victor plate reader (Wallac) with a time delay at 665 nm. cSrc assays contained: 0.4 nM Enzyme, 100 mM HEPES, and 100 nM peptide substrate

[Biotin-(6-amino caproic acid)-AAAQIYGGI-NH<sub>2</sub>; Quality Controlled Biochemicals, Inc.]. The reaction was allowed to proceed for 40 min, and product was detected using the HTRF procedure. CDK1 and CDK2 assays contained: 100 mM HEPES (pH 7.5), 10 mM  $MgCl_2$ , 0.1% BSA, 0.5  $\mu$ Ci of [ $\gamma$ - $^{33}P$ ]ATP, 1.4  $\mu$ M ATP (2  $\mu$ g/ml), CDK1 (1  $\mu$ g/ml), and CDK2, and 1.5  $\mu$ M Biotin-amino hexyl-ARRPMSPKKKA-CONH<sub>2</sub> (Quality Controlled Biochemicals, Inc). Reactions were initiated as described above and allowed to proceed for 30 min. Reactions were terminated with 100  $\mu$ l of 50 mM HEPES (pH 7.5) and 100 mM EDTA and allowed to proceed for 20 (CDK2) or 60 min (CDK1). Reactions were terminated by the addition of 20  $\mu$ l of 250 mM EDTA in PBS 7.0. Next, 180  $\mu$ l of Streptavidin SPA beads (Amersham) were added, the plates were sealed, and the beads were allowed to settle for at least 8 h, then the plate was counted.

Tie-2 was reactivated by incubation in the presence of 2 mM ATP, 5 mM  $MgCl_2$ , 12.5 mM DTT, and 0.1 M HEPES (pH 7.5) at room temperature for 30 min before it was diluted properly to make up the enzyme mixture. Tie-2 assays contained: 1  $\mu$ M Biotin-C6-LEARLVAYEGWVAGKKKamide (Synpep Corp.), 80  $\mu$ M ATP, 0.05 mM BSA, 100 mM HEPES (pH 7.5), 10 mM  $MgCl_2$ , 1 mM DTT, and 10 nM Tie-2. Product was detected using HTRF as described above.

MEK-6 and p38 were expressed and purified in an *Escherichia coli* expression system. MEK6-activated p38 was purified, and its ability to phosphorylate Biotin-IPTSPITTTY-FFFFRRR-amide (Quality Controlled Biochemicals, Inc.) in the presence or absence of GW2016 was measured in a scintillation proximity assay. p38 assays contained: 100 mM HEPES (pH 7.5), 10 mM  $Mg(C_2H_3O_2)_2$ , 0.08  $\mu$ Ci/well [ $\gamma$ - $^{33}P$ ]ATP, 1.5  $\mu$ M ATP, 1.5  $\mu$ M Biotin-IPTSPITTTYFFFFRRR-amide, 120 nM MEK6-activated p38, and 6% DMSO. Reactions were allowed to proceed for 60 min at room temperature and quenched with the addition of 50  $\mu$ l of 250 mM EDTA and mixed with 150  $\mu$ l of avidin SPA beads (Amersham) to 0.5 mg/reaction. The plates were sealed, and the beads were allowed to settle overnight. The plates were counted in a Packard TopCount for 60 s.

The ability of GW2016 to inhibit the c-Raf-1, MEK, and extracellular signal-regulated kinase cascade was determined as described previously (14).

**Cells and Cell Culture.** Normal HFFs were isolated by digesting human neonatal foreskins with a solution of 2.5% trypsin and 1 mM EDTA. The LICR-LON-HN5 head and neck carcinoma cell line (HN5) was a gift from Helmut Modjtahedi at the Institute of Cancer Research, Surrey, United Kingdom. The breast carcinoma cell lines, BT474, MCF-7, and T47D; the vulva carcinoma cell line, A-431; and the gastric carcinoma cell line, NCI-N87 (N87); were obtained from the American Type Culture Collection (Rockville, MD). HFF, HN5, and N87 were maintained by subculturing in 75-cm<sup>2</sup> tissue culture flasks in low-glucose DMEM containing 10% FBS (Hyclone) until ready for use. MCF-7 cells were maintained in high-glucose DMEM containing 10% FBS. BT474 cells were maintained in either DMEM or RPMI 1640 supplemented with 10% FBS. T47D, A-431, and CaLu-3 cells were maintained in RPMI supplemented with 10% FBS. HB4a and HB4a c5.2 cells were generated as described (15) and were maintained

in RPMI 1640 supplemented with 10% FBS, 5  $\mu\text{g/ml}$  hydrocortisone, 5  $\mu\text{g/ml}$  insulin, and 50  $\mu\text{g/ml}$  hygromycin B.

**Immunoprecipitation and Western Blot Analysis.** Cells were plated in 150-cm<sup>2</sup> tissue culture plates in the appropriate growth medium (BT474 = RPMI, HN5 = DMEM containing 10% FBS). When cells were in logarithmic growth (40–80% confluence), growth medium was aspirated and replaced with the appropriate growth medium containing either vehicle (0.1% DMSO), 0.03, 0.1, 0.3, 1, 3, or 10  $\mu\text{M}$  GW2016. Treated cells were returned to the incubator for 6 h. The medium was then removed, and cells were rinsed once with cold PBS (#14190–144; Life Technologies, Inc., Grand Island, NY) and lysed in 1 ml of RIPA [150 mM NaCl, 50 mM Tris-HCl (pH 7.5), 0.25% deoxycholate, and 1% NP-40] containing protease inhibitor cocktail (Roche) and 1 mM sodium orthovanadate (RIPA+).

EGFR was immunoprecipitated from 0.25 mg of HN5 lysate or 1 mg of BT474 lysate. HN5 and BT474 lysates were diluted to 0.75 and 1 ml, respectively, with RIPA+ and were precleared with 30  $\mu\text{l}$  of Protein G Plus/Protein A agarose suspension for 30 min at 4°C. Precleared lysates were transferred to new tubes, and 4 (for HN5) or 10  $\mu\text{l}$  (for BT474) of anti-EGFR Ab-13 (Lab Vision) were added. Tubes were incubated at 4°C for  $\geq 2$  h to allow complex formation. Protein G Plus/Protein A (30 ml) was added to each tube, and samples were incubated overnight at 4°C. Beads were spun down and washed once with RIPA, once with RIPA containing 0.1% SDS (RIPA-SDS), and once with PBS. Beads were resuspended in 20  $\mu\text{l}$  of SDS-PAGE sample buffer.

ErbB-2 was immunoprecipitated from 0.25 mg of BT474 lysate or 1 mg of HN5 lysate, diluted with 0.75 or 1 ml RIPA+, respectively, and precleared as described above. Precleared lysates were transferred to new tubes, and 4 (for BT474) or 10  $\mu\text{l}$  (for HN5) of anti-c-neu Ab-3 (Oncogene Research Products) were added. Complex formation, precipitation, and washes were carried out as described above.

Samples were boiled for 5 min before being loaded on 6% NOVEX gels (1.5 mm, 15 lanes). After electrophoresis, samples were transferred to nitrocellulose using standard Western blotting procedures, and the nitrocellulose membranes were blocked in TBST [150 mM NaCl, 10 mM Tris-HCl, and 0.1% (v/v) Tween 20 (pH 7.5)] containing 4% (w/v) BSA. Membranes were incubated in anti-pTyr monoclonal antibody PT66 (Sigma Chemical Co.) diluted 1:5000 in the TBST/BSA blocking buffer for 1–2 h at room temperature or overnight at 4°C. They were then rinsed twice in TBST, followed by three 20-min washes. Next, membranes were incubated in horseradish-peroxidase-conjugated antimouse secondary antibody diluted 1:100,000 (Jackson Immunoresearch) in TBST/BSA blocking buffer for 1 h at room temperature or overnight at 4°C. The membranes were washed as described above and were incubated in SuperSignal West Femto Detection Reagent (supplier) for 1 min. After blotting dry, membranes were placed in a sheet protector and exposed to film.

For densitometric analysis of EGFR and ErbB-2 phosphorylation, films were scanned on a Bio-Rad Fluor-S Multi-Imager, and relevant bands were quantified using Quantity One quantitation software. Concentrations that inhibit 50% of tyrosine phosphorylation ( $\text{IC}_{50}$ ) were interpolated using the

method of Levenberg and Marquardt (16) and this equation:  $y = V_{\text{max}} \times [1 - (x^n/(K^n + x^n))]$ , where “K” is equal to  $\text{IC}_{50}$ .

For phosphoserine AKT immunoblotting, the RIPA+ lysates described above (20  $\mu\text{g}$  of total protein) were run on 10% Tris-glycine gels (Novex/Invitrogen), transferred to nitrocellulose, blotted with an antiphospho-AKT-Ser (473) antibody (cat # 9271; Cell Signaling Technology), and diluted 1:1000 in 1% milk/TBST. Membranes were washed in TBST as described above and blotted with horseradish peroxidase-conjugated donkey antirabbit secondary antibody, diluted 1:10,000 in 1% milk/TBST. The membranes were washed again, as described above, and detection was performed with enhanced chemiluminescence (Amersham) using the method recommended by the manufacturer.

**In Vitro Growth Inhibition Assays.** For assessment of cell-based potency, cells were plated in 96-well Falcon plates (Becton Dickinson) in the growth media described above. Plating densities that resulted in logarithmic growth of vehicle-treated cells for the duration of the assay were used: HFF, 15,000 cells/cm<sup>2</sup>; BT474, MCF-7, N87, and CaLu-3, 30,000 cells/cm<sup>2</sup>; and HN5, A-431, T47D, HB4a, and HB4a c5.2, 10,000 cells/cm<sup>2</sup>. After 24 h, cells were exposed to compounds at the concentrations indicated in Fig. 2. HFF, BT474, HN5, and N87 cells were treated in low-glucose DMEM containing 5% FBS, 50  $\mu\text{g/ml}$  gentamicin, and 0.3% v/v DMSO. MCF-7 cells were treated in 50% high-glucose DMEM, 50% low-glucose DMEM containing 5% FBS, 50  $\mu\text{g/ml}$  gentamicin, and 0.3% v/v DMSO. T47D, A-431, and CaLu-3 cells were treated in 50% RPMI, 50% low-glucose DMEM containing 5% FBS, 50  $\mu\text{g/ml}$  gentamicin, and 0.3% v/v DMSO. HB4a and HB4a c5.2 cells were treated in 50% DMEM, 50% RPMI 1640 supplemented with 5% FBS, 2.5  $\mu\text{g/ml}$  hydrocortisone, 2.5  $\mu\text{g/ml}$  insulin, 25  $\mu\text{g/ml}$  hygromycin B, 50  $\mu\text{g/ml}$  gentamicin, and 0.3% v/v DMSO. After 3 days, relative cell number was estimated using methylene blue staining. The media were removed, and 100  $\mu\text{l}$  of 0.5% w/v methylene blue dissolved in 50% ethanol and 50% water were added to each well. Plates were washed by immersion in deionized water and allowed to air dry. 1% w/v n-lauroylsarcosine (100  $\mu\text{l}$ ) dissolved in PBS was added to each well, and plates were incubated for 30 min at room temperature. The absorbance at 620 nm was read in a Spectra (Tecan) microplate reader. Data were analyzed using curve-fitting macros written for Microsoft Excel. Concentrations with  $\text{IC}_{50}$  were interpolated using the method of Levenberg and Marquardt and this equation:  $y = V_{\text{max}} \times [1 - (x^n/(K^n + x^n))]$ , where “K” is equal to  $\text{IC}_{50}$ .

**Outgrowth Assays.** Cells were plated in 96-well plates, in the media described above, at the following densities: HFF and HN5, 1000 cells/well and BT474, 5000 cells/well. After 24 h, the cells were exposed to vehicle (0.3% DMSO) or GW2016 as described above, at the concentrations indicated in Fig. 3. Compound was removed from the cells after 72 h and was replaced by either DMEM containing 10% FBS and 50  $\mu\text{g/ml}$  gentamicin (HFF and HN5) or RPMI containing 10% FBS and 50  $\mu\text{g/ml}$  gentamicin (BT474). Methylene blue staining as described above was performed at the time points indicated in Fig. 3 over a total period of 16 days.



**Cell Cycle Analysis.** BT474 and HN5 cells were plated in six-well tissue culture plates at  $2 \times 10^6$  (BT474) and  $1 \times 10^5$  (HN5) cells/well. After 24 h, cells were treated with vehicle (0.1% DMSO) or GW2016 at the concentrations indicated. After 3 days of compound exposure, cells were labeled for 1 h with  $10 \mu\text{M}$  BrdUrd, rinsed with PBS, and harvested by trypsinization. The PBS and trypsin rinses were reserved and combined with the trypsinized cells. Cells were pelleted by centrifugation at  $500 \times g$  for 5 min. Supernatant was aspirated, and pellets were dissociated by vortexing and fixed by dropwise addition of ice-cold 70% methanol while vortexing. Cell death and cell cycle analysis were assessed by propidium iodide staining and antibody detection of incorporated BrdUrd and staining with propidium iodide according to the manufacturer's directions (Becton Dickinson).

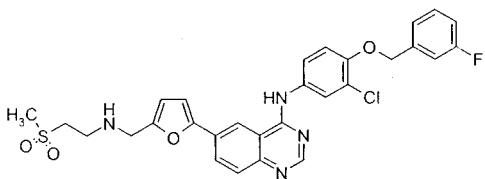
**In Vivo Studies.** CD-1 nude female mice and C.B-17 SCID female mice (4–6 weeks old) were purchased from Charles River Laboratories (Wilmington, MA) and housed in microisolator cages. The research complied with national legislation and with company policy on the Care and Use of Animals and with related codes of practice. All animal handling was done in a laminar flow hood. CD-1 nude female mice were used for HN5 human tumor xenografts, which were initiated by injection of a cell suspension in PBS:Matrigel (1:1). C.B-17 SCID female mice were used for BT474 human tumor xenografts, which were initiated by implantation of tumor fragments (20–100 mg) from established tumors. Tumor cells and fragments were implanted by s.c. injection in the right flank. The s.c. tumors were measured with calipers, and mice were weighed twice weekly. Tumor weight was estimated from tumor volume using this formula:  $\text{length} \times \text{width}^2/2 = \text{tumor volume (mm}^3\text{)}$ . Treatment began when tumors were palpable, ~3–5 mm in diameter. Experimental compounds were administered p.o. twice daily for 21 days in a vehicle of sulfo-butyl-ether- $\beta$ -cyclodextrin 10% aqueous solution (CD10).

## Results

**In Vitro Inhibition of Kinase Activity by GW2016.** Table 1 contains the structure and  $\text{IC}_{50}$  values for the inhibition of enzyme activity for GW2016. GW2016 is a 4-anilino, 6-substituted quinazoline with potent activity against both EGFR and ErbB-2 *in vitro*. The  $\text{IC}_{50}$  values for inhibition of enzyme activity were generated by measuring inhibition of phosphorylation of a peptide substrate. With the exception of ErbB-4, GW2016 was >300-fold selective for EGFR and ErbB-2 over other kinases tested.

**Inhibition of Receptor Autophosphorylation in Cells.** The ability of GW2016 to inhibit the activity of EGFR and ErbB-2 in intact cells was assessed by immunoprecipitation and Western blot analysis (Fig. 1). Receptor phosphorylation and protein levels were measured in HN5 and BT474 cells after 6 h of compound exposure. Receptors were immunoprecipitated using either EGFR or ErbB-2 antibodies and blotted for phosphotyrosine content. Treatment with GW2016 inhibited receptor autophosphorylation of EGFR and ErbB-2 in a dose-responsive manner. Averaged  $\text{IC}_{50}$  values are presented in Table 2. Expression of EGFR or ErbB-2 protein was not inhibited (data not shown). The ability

Table 1 Structure and enzyme inhibitory activity of GW2016

GW2016	
 <p style="text-align: center;">N-{3-Chloro-4-[(3-fluorobenzyl)oxy]phenyl}-6-[5-({2-(methylsulfonyl)ethyl}amino)methyl]-2-furyl]-4-quinazolinamine</p>	
Enzyme Inhibition	
Enzyme	$\text{IC}_{50}$ (nM)
EGFR	10.8 +/- 0.53
ErbB-2	9.2 +/- 0.75
ErbB-4	367 +/- 4.2
c-Src	3,500 +/- 650
c-Raf-1	> 10,000*
MEK	> 10,000*
ERK	> 10,000*
c-Fms	> 10,000*
CDK1	> 10,000
CDK2	> 10,000
p38	> 10,000
Tie-2	> 10,000*
VEGFR-2	> 10,000

<sup>a</sup>  $\text{IC}_{50}$  values were generated from 10-point dose-response curves (except where noted \*) and are presented with the SE.

<sup>b</sup> Treatment of these enzymes with a single dose of  $10 \mu\text{M}$  GW2016 resulted in <50% inhibition of enzyme activity.

of GW2016 to inhibit EGFR and ErbB-2 autophosphorylation in EGFR- and ErbB-2-overexpressing tumor cells is ~10-fold less than its potency on the purified enzyme. This effect has precedent with reversible quinazoline tyrosine kinase inhibitors (2, 16) and is likely attributable to competition for intracellular levels of ATP.

**In Vitro Growth Inhibition.** The ability of GW2016 to inhibit the growth of human tumor cells was assessed in a cell-based proliferation assay using protein staining as an estimate of relative cell number (Fig. 2 and Table 3). The cell-based assay included EGFR-overexpressing cell lines HN5 (17) and A-431 (18); the ErbB-2-overexpressing cell lines BT474 (19), N87 (20), and CaLu-3 (21); and tumor cell lines expressing low levels of EGFR and ErbB-2, MCF-7 (22), and T47D (23). The  $\text{IC}_{50}$  values were interpolated from 10-point dose-response curves using Levenberg-Marquardt nonlinear regression. Treatment with GW2016 resulted in  $\text{IC}_{50}$  values of  $\leq 0.16 \mu\text{M}$  on the EGFR- and the ErbB-2-overexpressing tumor cell lines. The ability of GW2016 to inhibit the growth of tumor cells overexpressing EGFR or ErbB-2 was compared with the EGFR selective inhibitors, OSI-774 and Iressa (Table 3). GW2016 inhibits the growth of

**Fig. 1.** Immunoprecipitation and Western blot analysis of receptor autophosphorylation in cells treated with GW2016. Cells were treated for 6 h with GW2016. Receptors were immunoprecipitated with antibodies to EGFR or ErbB-2 and blotted for phosphotyrosine. This representative Western blot shows that GW2016 inhibited phosphorylation of EGFR and ErbB-2 in a dose-responsive manner in the BT474 and HN5 cell lines.

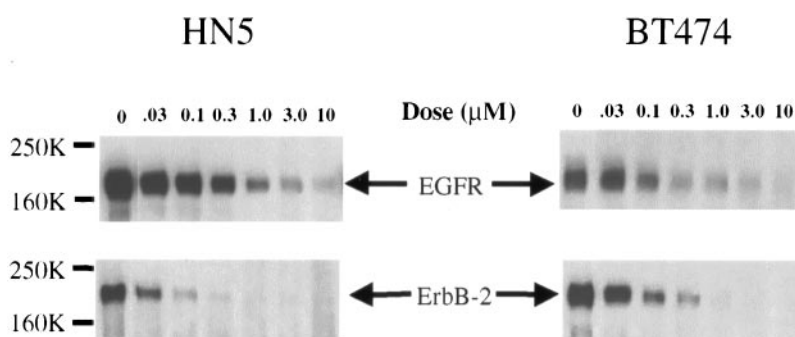


**Table 2** The  $IC_{50}$  values for inhibition of receptor tyrosine phosphorylation<sup>a</sup>

Cell line	Immunoprecipitated receptor <sup>b</sup>	Phosphotyrosine inhibition <sup>c</sup> ( $IC_{50}$ $\mu M$ )
BT474	EGFR	$0.17 \pm 0.03$
	ErbB-2	$0.08 \pm 0.02$
HN5	EGFR	$0.21 \pm 0.06$
	ErbB2	$0.06 \pm 0.03$

<sup>a</sup> Cells were treated for 6 h with GW2016.

<sup>b</sup> Receptors were immunoprecipitated and subjected to western blot analysis for phosphotyrosine content as described in "Materials and Methods."

<sup>c</sup> Relative phosphotyrosine content was quantified by laser densitometry from five or six point dose-response curves. Average  $IC_{50}$  values from four individual experiments are presented with the SE.

both EGFR- and ErbB-2-overexpressing cells, whereas OSI-774 and Iressa preferentially inhibit the growth of the EGFR-overexpressing cell lines. When compared with EGFR- and ErbB-2-overexpressing cell lines, GW2016 was less effective at inhibiting the growth of breast tumor cell lines expressing low levels of EGFR and ErbB-2, MCF-7, and T47D.  $IC_{50}$  values for these cell lines were  $\sim 3 \mu M$  and were  $\sim 25$ -fold higher than  $IC_{50}$  values for the EGFR- or ErbB-2-overexpressing cell lines. Selectivity for tumor *versus* normal tissue was determined by comparing efficacy of GW2016 on tumor cells to efficacy on HFF cells. Using the average of the tumor cell  $IC_{50}$  values, GW2016 is  $\sim 100$ -fold more potent on the tumor cell lines than on the normal fibroblast cells.

The selectivity for GW2016 on transfected *versus* normal epithelial cells was verified in a transfected cell system (Table 3 and Fig. 3). The ErbB-2-transfected mammary epithelial cell line, HB4a c5.2, is  $\sim 40$ -fold more responsive to GW2016 treatment than the untransfected parental control line, HB4a.

**Outgrowth Assays.** To determine concentrations of GW2016 capable of causing irreversible growth arrest of tumor cell populations, studies using transient exposure to GW2016 followed by outgrowth in the absence of compound were performed (Fig. 4). Cells were exposed to compound at the concentrations indicated for 3 days, followed by outgrowth in the absence of compound for 12 days. In multiple experiments, concentrations were reached where outgrowth after transient drug exposure did not occur. Transient exposure to  $30 \mu M$  GW2016 results in complete inhibition of outgrowth of the HN5 cell population after  $\sim 2$  additional weeks of culture without compound. Inhibition of outgrowth

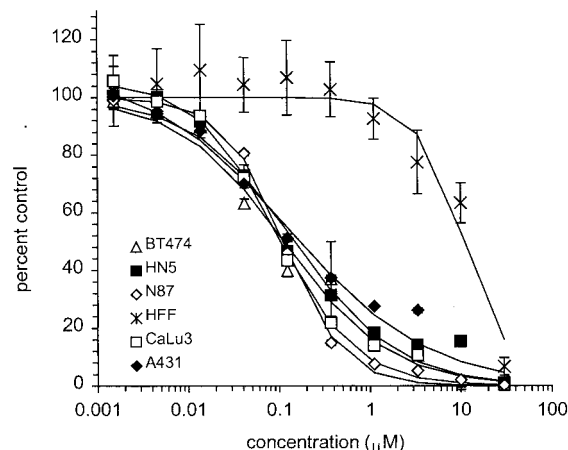


**Fig. 2.** Selective inhibition of the proliferation of human tumor cell lines compared with normal cells by GW2016. The representative dose-response curves show that GW2016 was effective against all of the ErbB-2- and EGFR-positive cell lines. Normal human fibroblasts were less sensitive to inhibition of ErbB-2 or EGFR with respect to cell proliferation. Relative cell number was estimated by methylene blue protein staining and plotted as a percentage of vehicle-treated control. Fitted lines were generated using 4-parameter nonlinear regression.

by 50% occurs at concentrations  $>3.3 \mu M$ . Significant inhibition of outgrowth (20%) occurs at doses as low as  $0.37 \mu M$  ( $P = 0.001$ ; Fig. 4a). Another EGFR-overexpressing cell line, A-431, responded similarly to HN5 (data not shown). GW2016 was similar to OSI-774 in its ability to inhibit outgrowth of the EGFR-overexpressing cell line (Fig. 4b).

The threshold for complete inhibition of the BT474 cells is  $1 \mu M$ , with  $\sim 60\%$  inhibition of outgrowth occurring at  $0.37 \mu M$  ( $P = 0.004$ ; Fig. 4c). Another ErbB-2-overexpressing cell line, N87, responded similarly to BT474 (data not shown). GW2016 is much more effective than OSI-774 at inhibiting the outgrowth of the ErbB-2-overexpressing cell lines (Fig. 4d). Normal fibroblasts are less responsive to GW2016 in the outgrowth assay than the EGFR- or ErbB-2-overexpressing cell lines. Outgrowth of the HFF cell line is not significantly inhibited at concentrations of GW2016  $<10 \mu M$  ( $\sim 10\%$  inhibition at  $3.3 \mu M$ ), and evidence of survival is seen at the  $30 \mu M$  (Fig. 4e).

**Cell Cycle.** The effect of GW2016 treatment on the cell cycle of EGFR- and ErbB-2-overexpressing cells was determined by flow cytometric analysis of BrdUrd incorporation

Table 3 The IC<sub>50</sub> values<sup>a</sup> (μM) for inhibition of cell growth by 72-h treatment with GW2016, Iressa, or OSI-774

Cell line	Relative expression <sup>b</sup>		GW2016	ZD1839	OSI-774
	EGFR	ErbB-2			
HFF	+	— <sup>c</sup>	12 ± 1.4	>10	>8.7
MCF-7	+	+	4.0 ± 0.1	14.2 ± 0.6	>30
T47D	+	+	3.0 ± 0.2	10.5 ± 0.5	14.5 ± 0.6
A-431	+++	+	0.16 ± 0.03	0.08 ± 0.02	0.10 ± 0.03
HN5	+++	+	0.12 ± 0.03	0.08 ± 0.01	0.18 ± 0.02
BT474	+	+++	0.10 ± 0.03	1.1 ± 0.1	9.9 ± 1.6
N87	+	+++	0.09 ± 0.02	2.6 ± 0.9	4.6 ± 0.5
CaLu-3	ND	+++	0.13 ± 0.03	ND	ND
HB4a	+	—	9.1 ± 0.8	14.5 ± 0.4	23.8 ± 2.1
HB4a c5.2	+	+++	0.21 ± 0.03	1.1 ± 0.4	1.8 ± 0.7

<sup>a</sup> The IC<sub>50</sub> values are averages of a minimum of two experiments and are presented with the SE.

<sup>b</sup> Relative EGFR and ErbB-2 protein expression of each cell line was confirmed by Western blot analysis or, in the case of A431, inferred from the literature (41).

<sup>c</sup> —, below detectable levels by Western blot; ND, not determined.

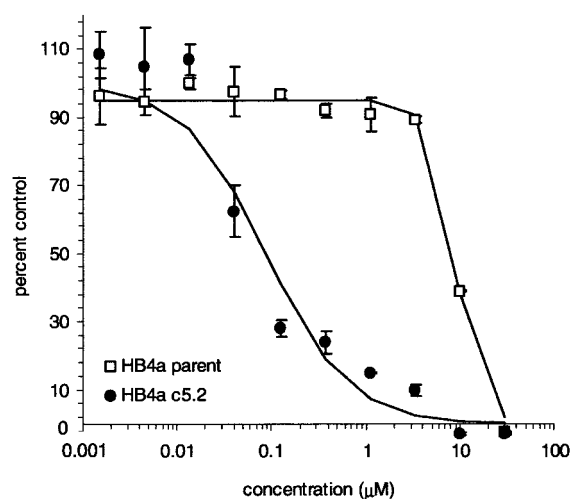


Fig. 3. Selective growth inhibition of ErbB-2-transfected epithelial cells. Parental HB4a mammary epithelial cells or the ErbB-2-transfected HB4a c5.2 clone was treated with GW2016 for 3 days at the concentrations indicated. The representative growth curves show that GW2016 was more effective at inhibiting the ErbB-2-transfected clone than the parental control cell line. Relative cell number was estimated by methylene blue protein staining and plotted as a percentage of vehicle-treated control. Fitted lines were generated using 4-parameter nonlinear regression.

and propidium iodide staining. Results are shown in Fig. 5 and Table 4. Treatment of the EGFR-overexpressing cell line, HN5, with 1 and 10 μM GW2016 resulted in induction of G1 arrest. A slight increase in the number of cells with sub-2N DNA content, consistent with cell death by an apoptotic mechanism, was also observed by 72 h with 10 μM GW2016. In the BT474 cells, a large increase in the number of events with sub-2N DNA was observed after 72 h of treatment with GW2016. Apoptosis was confirmed by the detection of disrupted nuclear fragments after staining methanol-fixed cells with 4',6-diamidino-2-phenylindole (data not shown).

**Effects on Signal Transduction.** To correlate the effects of GW2016 on cell growth and survival with specific biochemical effects, we investigated the ability of the compound to inhibit the phosphorylation of key signal transduction mediator AKT (Fig. 6). AKT phosphorylation has been linked to

inhibition of apoptotic pathways and, thus, cell survival in a number of systems (1, 24–26). Western blot analysis using a phosphorylation state-specific AKT antibody shows that GW2016 inhibits the phosphorylation AKT in both of the cell lines tested. Although EGFR and ErbB-2 are inhibited similarly in the BT474 and HN5 cells, there are dramatic differences between the amount of inhibition of AKT phosphorylation in response to 6 h of GW2016 treatment. AKT phosphorylation is inhibited to a much greater extent in the BT474 cells than in the HN5 cells, correlating with the ability of GW2016 to initiate cell death (BT474) or growth arrest (HN5) in these cell lines.

**Xenograft Growth Inhibition.** GW2016 was potent at inhibiting the growth of BT474 and HN5 human tumor xenografts (Fig. 7). A dose-responsive inhibition of both models occurred on treatment of tumor-bearing mice with 30 and 100 mg/kg GW2016 orally, twice daily. Complete inhibition of tumor growth was seen at the 100 mg/kg dose. At this dose, there was <10% weight loss in treated animals over the course of the 21-day treatment (data not shown).

## Discussion

GW2016 is a potent inhibitor of EGFR and ErbB-2 kinase activity. Using *in vitro* cell-based assays and tumor xenograft models, we sought to determine whether GW2016 has potential use in anticancer therapy. We tested GW2016 in the BT474, HN5, N87, CaLu-3, and A-431 tumor cell lines. The BT474, HN5, and A-431 tumor models have proven reliable predictors of compound activity for type I receptor-targeted therapies that have advanced to the clinical setting. These include the currently approved cancer therapy, Herceptin (27, 28), and the small molecule inhibitors OSI-774 (2, 7), Iressa (29), and CI 1033 (30), which are currently in clinical trials.

The data show that GW2016 is potent at inhibiting the growth of a number of EGFR- and ErbB-2-overexpressing cell lines from a variety of tumor types, including the validated models mentioned above. The ability of GW2016 to inhibit the growth of EGFR-overexpressing cell lines is equal to that of the EGFR selective inhibitors, OSI-774 and Iressa. As expected, GW2016 is able to inhibit the growth of ErbB-

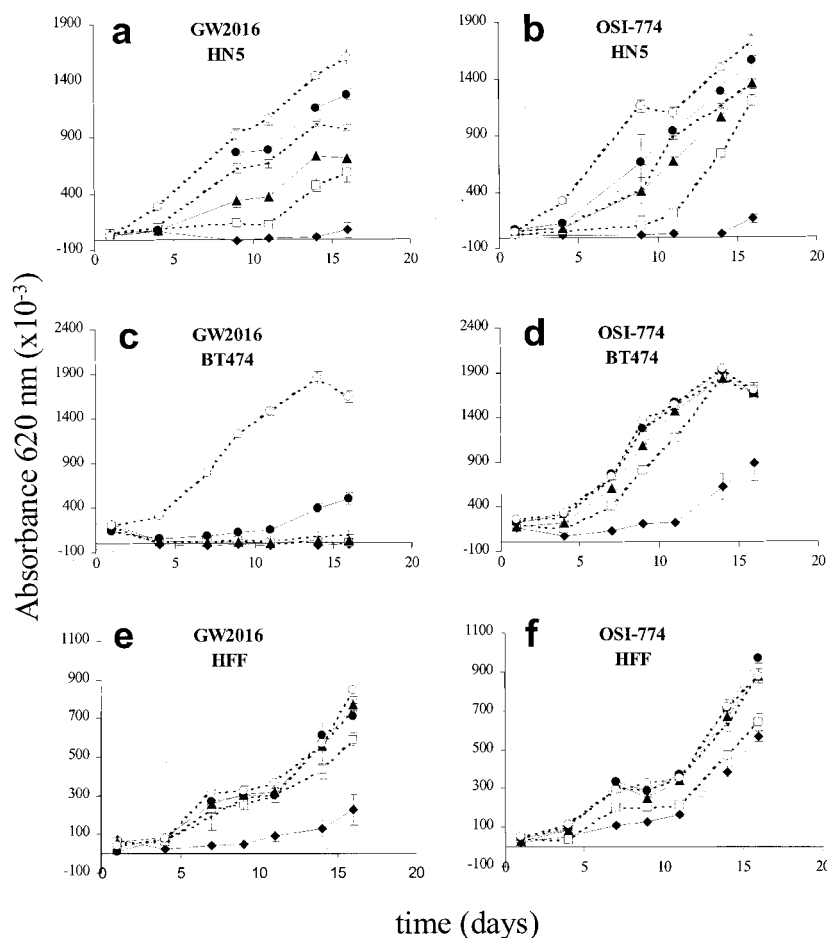


**Fig. 4.** Growth arrest or cell death in EGFR- or ErbB-2-overexpressing cells caused by treatment with GW2016. Cells were treated for 3 days with GW2016 or OSI-774 (an EGFR-selective inhibitor, used as a positive control), beginning on day 1. GW2016 (or OSI-774) was removed on day 4 and replaced with fresh growth medium. Cells were fed weekly for the duration of the assay. Methylene blue staining was performed at the time points indicated on the graph. Doses of GW2016 resulting in inhibition outgrowth after 3 days of drug exposure were achieved cells that overexpress EGFR (HN5) and ErbB-2 (BT474). Vehicle  $\circ$ — $\circ$ , 0.37  $\mu$ M  $\bullet$ — $\bullet$ , 1.1  $\mu$ M  $\square$ — $\square$ , 3.3  $\mu$ M  $\blacktriangle$ — $\blacktriangle$ , 10  $\mu$ M  $\square$ — $\square$ , and 30  $\mu$ M  $\blacklozenge$ — $\blacklozenge$ .

2-overexpressing cell lines with more potency than the EGFR-selective inhibitors tested. These and previous data suggest that an inhibitor of both EGFR and ErbB-2 could provide benefit to a wider population of cancer patients than therapies targeted to EGFR or ErbB-2 alone, by including patients expressing high levels of either receptor.

It is generally considered advantageous for anticancer therapy to eliminate cancer cells by differentiation or death as opposed to causing reversible growth arrest (31). Much has been speculated about the ability of type I receptor inhibitors to cause cell cycle arrest *versus* cell death. Inhibition of EGFR has been linked to both reversible growth arrest (32, 33) and entry into apoptosis (2, 17) in various models. Treatment of cells in culture with ErbB-2 mediators has predominantly been shown to cause reversible growth arrest (34, 35). However, cell death has been shown to occur on abrogation of ErbB-2 signaling by an antisense oligonucleotide (36) or ribozyme (37). Furthermore, EGFR and ErbB-2 activation have been linked to the PI3K/AKT cell survival pathway, implying that inhibition of EGFR or ErbB-2 catalytic activity should be capable of inducing cell death. We used outgrowth studies to test the ability of transient treatment with GW2016 to inhibit the growth of tumor and normal cells. These studies confirm that above certain concentrations of

GW2016, EGFR- and ErbB-2-overexpressing tumor cells cannot continue to proliferate, even after removal of compound. Cell cycle analysis corroborated the outgrowth studies. Evidence of cell death was seen with doses of GW2016 that reduced outgrowth potential in the HN5 and BT474 cell lines.

In the outgrowth and cell cycle assays that we performed, GW2016 proved more effective against ErbB-2-overexpressing cell lines than against EGFR-overexpressing cell lines. We do not know if this differential effect applies to EGFR-overexpressing cell lines in general or if it is unique to the cell lines tested in this study. The data presented suggest that inhibition of EGFR by GW2016 results preferentially in cell growth arrest, whereas inhibition of ErbB-2 yields growth arrest and cell death after 72 h *in vitro*.

The inhibition of AKT phosphorylation in the two cell lines provides interesting insight into the differential response of the EGFR- and ErbB-2-overexpressing cells to GW2016. The ability of GW2016 treatment of the EGFR-overexpressing cell line, HN5, to down-regulate AKT phosphorylation is limited until concentrations reach 3  $\mu$ M. HN5 cells primarily undergo reversible growth arrest rather than apoptosis after treatment with GW2016; however, at 10  $\mu$ M GW2016, there is a significant but incomplete inhibition of outgrowth of the HN5 cells.



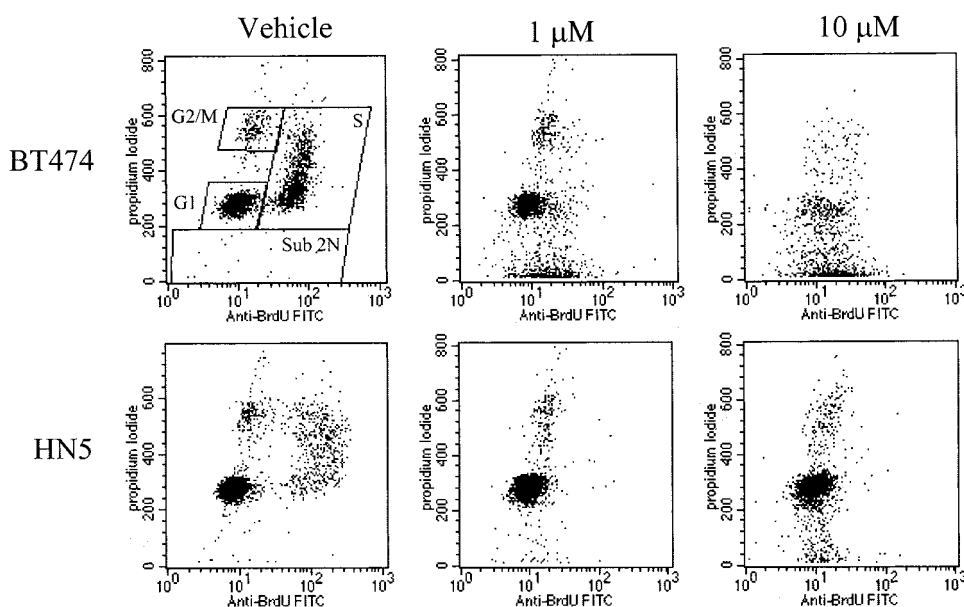


Fig. 5. Cell cycle effects of GW2016. Cells were exposed to GW2016 at the indicated doses for 3 days. Cell cycle status and amount of cell death were estimated using BrdUrd incorporation and propidium iodide staining. GW2016 treatment resulted in G1 arrest in cells overexpressing EGFR (HN5) or ErbB-2 (BT474). An increase in the amount of cells staining with sub-2N amounts of DNA in both EGFR- and ErbB-2-overexpressing cells is consistent with cell death by apoptosis. Treatment with GW2016 resulted in the death of more BT474 than HN5 cells.

Table 4 Cell cycle effects<sup>a</sup> and induction of apoptosis<sup>b</sup> by GW2016<sup>c</sup>

Cell line	Phase	Vehicle control	1 $\mu\text{M}$ GW2016	10 $\mu\text{M}$ GW2016
BT474	G1	50	70	28
	S	37	1	2
	G2/M	9	8	8
	Apoptosis (Sub-2N DNA)	1	18	57
HN5	G1	51	91	79
	S	39	2	1
	G2/M	8	4	9
	Apoptosis (Sub-2N DNA)	1	1	8

<sup>a</sup> Values were determined by gate analysis of flow cytometric plots in Fig. 5 and are presented as a percentage of the total cell population, after eliminating cell doublets. The addition of values for each treatment do not total 100% attributable to the presence of a small population of events appearing outside of the normal cell cycle.

<sup>b</sup> Apoptotic events are inferred by the presence of cells with <2N DNA.

<sup>c</sup> Cells were treated for 72 h, followed by flow cytometric analysis.

This is consistent with the ability of GW2016 to induce a low level of apoptosis and reversible growth arrest in this cell line. The cell cycle and outgrowth assay results correspond with the ability of GW2016 to inhibit phosphorylation of AKT in the HN5 cells only at a dose  $\geq 3 \mu\text{M}$ . Outgrowth studies in the EGFR-overexpressing A431 cell line are similar to the HN5 response. The ErbB-2-overexpressing cell line, BT474, dramatically down-regulates AKT phosphorylation in response to GW2016 treatment at doses as low as  $0.3 \mu\text{M}$ . BT474 cells undergo apoptosis after 72 h of GW2016 treatment at 1 or  $10 \mu\text{M}$ . Outgrowth of the BT474 cell line is inhibited significantly at doses as low as  $0.37 \mu\text{M}$ . Outgrowth assays with another ErbB-2-overexpressing cell line, N87, yielded similar results to the BT474 outgrowth assays. Therefore, ErbB-2-overexpressing tumor cell lines may be highly susceptible to apoptosis on abrogation of receptor activity.

These results are consistent with the finding that inhibition of AKT phosphorylation in the presence of activated p38 is a key mediator of apoptosis after treatment with the irrevers-

ible type I receptor inhibitor, CI 1033 (30). Indeed, we show potent down-regulation of AKT phosphorylation in the BT474 cell line, correlating with a considerable induction of apoptosis. Interestingly, the HN5 cell line is growth inhibited by GW2016 with less dramatic effects on AKT phosphorylation. It is possible that mechanisms for activating p38 are not in place in the HN5 cells, thus preventing complete inhibition of AKT activity and maintaining activation of certain AKT-dependent cell survival pathways. The fact that the  $\text{IC}_{50}$  for HN5 cell growth is the same as BT474 in the 72-h proliferation assay implies the interruption of an EGFR-dependent proliferation signal in the HN5 cells. Given the interplay between the type I receptors and the PI3K, ras, c-Jun-NH<sub>2</sub>-terminal kinase, and signal transducers and activators of transcription pathways (38, 39), the potential exists for complex interactions which could affect the response of tumors to type I receptor therapy. Unique signaling in EGFR- versus ErbB-2-overexpressing cells should continue to be investigated, with the appreciation that the effects of type I receptor inhibition could also be greatly influenced by the relative levels of the other family members, ErbB-3 and ErbB-4 (40). Furthermore, extensive testing of GW2016 in a variety of cellular systems and investigation of multiple downstream mediators of type I receptors must be completed to define the specific effects of this compound on ErbB-2- or EGFR-overexpressing tumors. Regardless of the intricacies of EGFR and ErbB-2 signaling in cell survival, we have shown that inhibition of either of these enzymes with GW2016 results in interference of growth or survival of cells from many tumor types, overexpressing either EGFR or ErbB-2.

One possible advantage of signal transduction inhibitors compared with conventional cytotoxic chemotherapy is that, by targeting specific molecular dysfunctions in cancer cells, the signal transduction inhibitors may be responsible for fewer side effects and adverse events. Therefore, it was necessary to demonstrate the selectivity of GW2016 for its



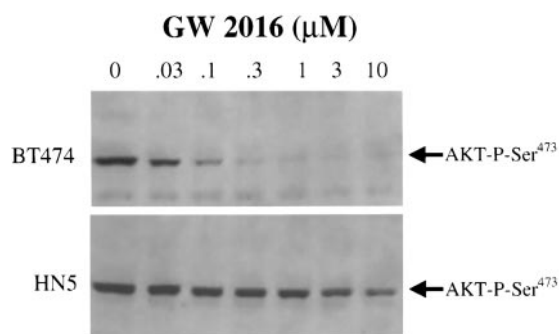


**Fig. 6.** Inhibition of AKT phosphorylation by GW2016. Cells were treated for 6 h with GW2016 at the concentrations indicated. Lysates were subjected to Western blot analysis using a phosphospecific AKT antibody. Phosphorylation of serine 473 of AKT was inhibited by GW2016 in a dose-dependent manner. The amount of AKT inhibition is greater in the BT474 cells than in the HN5 cells.

molecular targets, EGFR and ErbB-2, and for tumor cells that are dependent on the EGFR and ErbB-2 signaling pathways. Attributable to the possibility of confounding results from interdependent signal transduction pathways, we performed selectivity experiments on purified enzymes. Data from *in vitro* assays show that GW2016 is >300-fold more potent on EGFR and ErbB-2 than a number of other kinases involved in cellular proliferation. Furthermore, we have shown previously that EGFR/ErbB-2 selective inhibitors specifically affect growth of HB4a breast epithelial cells transfected with *erbB-2* as compared with *Ha-ras* transfected HB4a cells (10). We present data that show GW2016 is selective for the *erbB-2*-transfected cell line relative to the untransfected parental control cell line. The *ras*-transfected cell line in this system is also much less responsive to GW2016 than the ErbB-2-transfected clone (data not shown). We also present evidence that tumor cells expressing low levels of EGFR and ErbB-2 (MCF-7 and T47D) are >25-fold less responsive to growth inhibition by GW2016. Because it was necessary to verify that GW2016 was inhibiting the EGFR and ErbB-2 kinases intracellularly, we confirmed that GW2016 inhibits the phosphorylation of EGFR and ErbB-2 by immunoprecipitation and Western blot analysis of EGFR and ErbB-2 in cells after treatment with various doses of GW2016. Taken together, these results suggest that the effects of GW2016 in cell growth assays are attributable to specific inhibition of EGFR and ErbB-2 kinase activity, verifying the selectivity of GW2016 and adding to the validation of EGFR and ErbB-2 as targets in anticancer therapy.

Potential cancer therapies must not only inhibit cell growth *in vitro* but must be able to inhibit tumor growth in the complex *in vivo* environment. We confirmed that GW2016 is capable of inhibiting the growth of human tumor cells *in vivo*, using HN5 and BT474 xenograft models. The ability of GW2016 to inhibit the HN5 tumor xenograft is similar to that reported for OSI-774 (7). GW2016 treatment can achieve tumor growth inhibition in the BT474 xenograft model that is similar to the efficacy of Herceptin monotherapy (28).

GW2016 is a novel inhibitor of EGFR and ErbB-2 kinase activity. In EGFR-overexpressing cell lines, the ability of GW2016 to inhibit growth is equal to that of small molecule

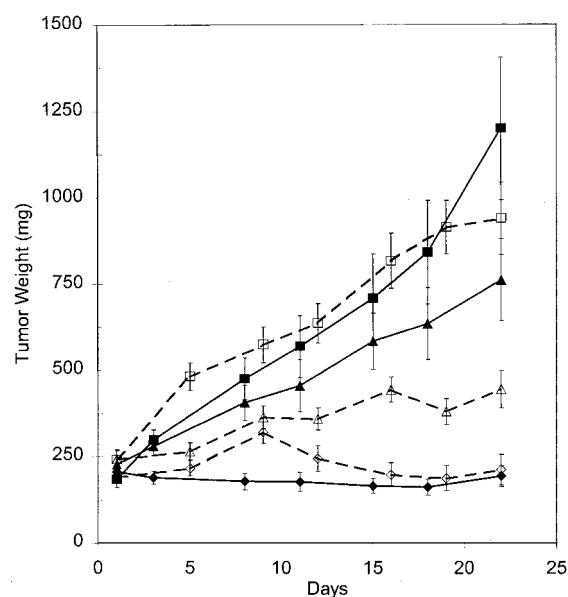


**Fig. 7.** Inhibition of tumor growth by GW2016. Cells or tumor fragments were implanted into immunocompromised mice. After establishment of tumors, animals were treated p.o. for 21 days on a twice-a-day schedule with GW2016 at the concentrations indicated. Tumors were measured with electronic calipers. □— HN5 Vehicle, △— HN5 30 mg/kg, ◇— HN5 100 mg/kg, ■— BT474 Vehicle, ▲— BT474 30 mg/kg, and ◆— BT474 100 mg/kg.

EGFR inhibitors presently in clinical trials. In ErbB-2-overexpressing cells, GW2016 is much more potent at inhibiting cell growth than are the EGFR inhibitor clinical candidates tested. Therefore, we believe that GW2016 has the potential to benefit cancer patients with tumors overexpressing either EGFR, ErbB-2, or both of these receptors together.

#### Acknowledgments

We thank Perry S. Brignola for providing purified EGFR, ErbB-2, and ErbB-4. We also thank Neal Bramson, Laurie Kane, Wendy Liu, Brad McDonald, Justin Mitchell, Frank Preugschat, Stephanie Schweiker, Darren Stuart, Gaochao Tian, Anne Truesdale, John Van Arnold, and Malcolm Willson for enzyme selectivity testing. Finally, we thank Jean Scott for editorial assistance in the preparation of this manuscript.

#### References

- Krasilnikov, M. A. Phosphatidylinositol-3 kinase dependent pathways: the role in control of cell growth, survival, and malignant transformation. *Biochemistry (Mosc)*. 65: 59–67, 2000.
- Moyer, J. D., Barbacci, E. G., Iwata, K. K., Arnold, L., Boman, B., Cunningham, A., DiOrio, C., Doty, J., Morin, M. J., Moyer, M. P., Neveu, M., Pollack, V. A., Pustilnik, L. R., Reynolds, M. M., Sloan, D., Theleman, A., and Miller, P. Induction of apoptosis and cell cycle arrest by CP-358,774, an inhibitor of epidermal growth factor receptor tyrosine kinase. *Cancer Res.*, 57: 4838–4848, 1997.
- Ciardello, F., Caputo, R., Bianco, R., Damiano, V., Pomatico, G., Placido, S. D., Bianco, A. R., and Tortora, G. Antitumor effect and potentiation of cytotoxic drugs activity in human cancer cells by ZD-1839 (Iressa), an epidermal growth factor receptor-selective tyrosine kinase inhibitor. *Clin. Cancer Res.*, 6: 2053–2063, 2000.
- Traxler, P. Tyrosine kinase inhibitors in cancer treatment (part II). *Expert Opinion on Therapeutic Patents*, 8: 1599–1625, 1998.
- Swaisland, H., Laight, A., Stafford, L., Jones, H., Morris, C., Dane, A., and Yates, R. Pharmacokinetics and tolerability of the orally active selec-

tive epidermal growth factor receptor tyrosine kinase inhibitor ZD1839 in healthy volunteers. *Clin. Pharmacol.*, *40*: 297–306, 2001.

6. Baselga, J., and Averbuch, S. D. ZD1839 (“Iressa”) as an anticancer agent. *Drugs*, *60*: 33–42, 2000.

7. Pollack, V. A., Savage, D. M., Baker, D. A., Tsaparikos, K. E., Sloan, D. E., Moyer, J. D., Barbaccini, E. G., Pustilnik, L. R., Smolarek, T. A., Davis, J. A., Vaidya, M. P., Arnold, L. D., Doty, J. L., Iwata, K. K., and Morin, M. J. Inhibition of epidermal growth factor receptor-associated tyrosine phosphorylation in human carcinomas with CP-358,774: dynamics of receptor inhibition *in situ* and antitumor effects in athymic mice. *J. Pharmacol. Exp. Ther.*, *291*: 739–748, 1999.

8. Smaill, J. B., Rewcastle, G. W., Loo, J. A., Greis, K. D., Chan, O. H., Reyner, E. L., Lipka, E., Showalter, H. D. H., Vincent, P. W., Elliott, W. L., and Denny, W. A. Tyrosine kinase inhibitors. 17 irreversible inhibitors of the epidermal growth factor receptor: 4-(phenylamino)quinazoline- and 4-(phenylamino)pyrido[3,2-d]pyrimidine-6-acrylamides bearing additional solubilizing functions. *J. Med. Chem.*, *43*: 1380–1397, 2000.

9. Cockerill, S., Stubberfield, C., Stables, J., Carter, M., Guntrip, S., Smith, K., McKeown, S., Shaw, R., Topley, P., Thomsen, L., Affleck, K., Jowett, A., Hayes, D., Willson, M., Woollard, P., and Spalding, D. Indolylamino quinazolines and pyridopyrimidines as inhibitors of EGFR and c-erbB-2. *Bioorg. Med. Chem. Lett.*, *11*: 1401–1405, 2001.

10. Rusnak, D. W., Affleck, K., Cockerill, S. G., Stubberfield, C., Harris, R., Page, M., Smith, K. J., Guntrip, S. B., Carter, M. C., Shaw, R. J., Jowett, A., Stables, J., Topley, P., Wood, E. R., Brignola, P. S., Kadwell, S. H., Reep, B. R., Mullin, R. J., Alligood, K. J., Keith, B. R., Crosby, R. M., Murray, D. M., Knight, W. B., Gilmer, T. M., and Lackey, K. The characterization of novel, dual ErbB-2/EGFR, tyrosine kinase inhibitors: potential therapy for cancer. *Cancer Res.*, *61*: 7196–7203, 2001.

11. Carter, M. C., Cockerill, G. S., Guntrip, S. B., Lackey, K. E., and Smith, K. J. Bicyclic heteroaromatic compounds [quinazolinamines and analogs] useful as protein tyrosine kinase inhibitors. PCT Int. Appl., WO9935146, Glaxo Wellcome, 1999.

12. Arnold, L., and Schnur, R. Alkynyl and azido-substituted 4-anilinoquinazoline derivatives are potent inhibitors of the erbB family of oncogenic and proto-oncogenic protein tyrosine kinase(s), useful for treating hyper-proliferative disorders. US Patent 5,747,498. Pfizer, Inc., 1998.

13. Gibson, K. H. Quinazoline Derivatives. US Patent 5,770,599. Zeneca Limited, 1998.

14. McDonald, O. B., Chen, W.-J., Ellis, B., Hoffman, C., Overton, L., Rink, M., Smith, A., Marshall, C. J., and Wood, E. R. A scintillation proximity assay for the Raf/MEK/ERK kinase cascade: high-throughput screening and identification of selective enzyme inhibitors. *Anal. Biochem.*, *268*: 318–329, 1999.

15. Harris, R. A., Eichholtz, T. J., Hiles, I. D., Page, M. J., and O’Hare, M. J. New model of erbB-2 over-expression in human mammary luminal epithelial cells. *Int. J. Cancer*, *80*: 477–484, 1999.

16. Woodburn, J. R. The epidermal growth factor receptor and its inhibition in cancer therapy. *Pharmacol. Ther.*, *82*: 241–250, 1999.

17. Modjtahedi, H., Affleck, K., Stubberfield, C., and Dean, C. EGFR blockade by tyrosine kinase inhibitor or monoclonal antibody inhibits growth, directs terminal differentiation and induces apoptosis in the human squamous cell carcinoma HN5. *Int. J. Oncol.*, *13*: 335–342, 1998.

18. Haigler, H., Ash, J., Singer, S., and Cohen, S. Visualization by fluorescence of the binding and internalization of epidermal growth factor in human carcinoma cells A-431. *Proc. Natl. Acad. Sci. USA*, *75*: 3317–3321, 1978.

19. Pasleau, F., Grootclaes, M., and Gol-Winkler, R. Expression of the *c-erbB2* gene in the BT474 human mammary tumor cell line: measurement of *c-erbB2* mRNA half-life. *Oncogene*, *8*: 849–854, 1993.

20. Batra, J. K., Kasprzyk, P. G., Bird, R. E., Pastan, I., and King, C. R. Recombinant anti-erbB2 immunotoxins containing *Pseudomonas* exotoxin. *Proc. Natl. Acad. Sci. USA*, *89*: 5867–5871, 1992.

21. Tagliabue, E., Centis, F., Campiglio, M., Mastroianni, A., Martignone, S., Pellegrini, R., Casalini, P., Lanzi, C., Menard, S., and Colnaghi, M. I. Selection of monoclonal antibodies which induce internalization and phosphorylation of p185<sup>HER2</sup> and growth inhibition of cells with HER2/*neu* gene amplification. *Int. J. Cancer*, *47*: 933–937, 1991.

22. Aguilar, Z., Akita, R. W., Finn, R. S., Ramos, B. L., Pegram, M. D., Kabbinnavar, F. F., Pietras, R. J., Pisacane, P., Sliwkowski, M. X., and Slamon, D. J. Biological effects of heregulin/*neu* differentiation factor on normal and malignant human breast and ovarian epithelial cells. *Oncogene*, *18*: 6050–6062, 1999.

23. Jannot, C. B., Beerli, R. R., Mason, S., Gullick, W. J., and Hynes, N. E. Intracellular expression of a single-chain antibody directed to the EGFR leads to growth inhibition of tumor cells. *Oncogene*, *13*: 275–282, 1996.

24. Datta, S. R., Brunet, A., and Greenberg, M. E. Cellular survival: a play in three Acts. *Genes Dev.*, *13*: 2905–2927, 1999.

25. Okano, J.-I., Gaslightwall, I., Birnbaum, M. J., Rustgi, A. K., and Nakagawa, H. Akt/Protein Kinase B isoforms are differentially regulated by epidermal growth factor stimulation. *J. Biol. Chem.*, *275*: 30934–30942, 2000.

26. Zhou, B. P., Hu, M. C.-T., Miller, S. A., Yu, Z., Xia, W., Lin, S.-Y., and Hung, M.-C. *HER-2/neu* blocks tumor necrosis factor-induced apoptosis via the Akt/NF- $\kappa$ B pathway. *J. Biol. Chem.*, *275*: 8027–8031, 2000.

27. Lane, H. A., Beuvink, I., Motoyama, A. B., Daly, J. M., Neve, R. M., and Hynes, N. E. ErbB2 potentiates breast tumor proliferation through modulation of p27<sup>KIP1</sup>-Cdk2 complex formation: receptor overexpression does not determine growth dependency. *Mol. Cell. Biol.*, *20*: 3210–3223, 2000.

28. Baselga, J., Norton, L., Albanell, J., Kim, Y. M., and Mendelsohn, J. Recombinant humanized anti-HER2 antibody (Herceptin) enhances the antitumor activity of paclitaxel and doxorubicin against HER2/*neu* overexpressing human breast cancer xenografts. *Cancer Res.*, *58*: 2825–2831, 1998.

29. Sirotnak, F. M., Zakowski, M. F., Miller, V. A., Scher, H. I., and Kris, M. G. Efficacy of cytotoxic agents against human tumor xenografts is markedly enhanced by coadministration of ZD1839 (Iressa), an inhibitor of EGFR tyrosine kinase. *Clin. Cancer Res.*, *6*: 4885–4892, 2000.

30. Nelson, J. M., and Fry, D. W. Akt, MAPK (ERK1/2), and p38 act in concert to promote apoptosis in response to ErbB receptor family inhibition. *J. Biol. Chem.*, *276*: 14842–14847, 2001.

31. Huang, P., and O’Liff, A. Signaling pathways in apoptosis as potential targets for cancer therapy. *Trends Cell Biol.*, *11*: 342–348, 2001.

32. Busse, D., Doughty, R. S., Ramsey, T. T., Russell, W. E., Price, J. O., Flanagan, W. M., Shawver, L. K., and Arteaga, C. L. Reversible G1 arrest induced by inhibition of the epidermal growth factor receptor tyrosine kinase requires up-regulation of p27<sup>KIP1</sup> independent of MAPK activity. *J. Biol. Chem.*, *275*: 6987–6995, 2000.

33. Fan, Z., and Mendelsohn, J. Therapeutic application of anti-growth factor receptor antibodies. *Curr. Opin. Oncol.*, *10*: 67–73, 1998.

34. Hudziak, R. M., Lewis, G. D., Winget, M., Fendly, B. M., Shepard, H. M., and Ullrich, A. p185<sup>HER2</sup> monoclonal antibody has antiproliferative effects *in vitro* and sensitizes human breast tumor cells to tumor necrosis factor. *Mol. Cell. Biol.*, *9*: 1165–1172, 1989.

35. Zhang, L., Lau, Y.-K., Xi, L., Hong, R.-L., Kim, D. S., Chen, C.-F., Hortobagyi, G. N., Chang, C.-J., and Hung, M.-C. Tyrosine kinase inhibitors, emodin and its derivative, repress Her-2/*neu*-induced cellular transformation and metastasis-associated properties. *Oncogene*, *16*: 2855–2863, 1998.

36. Roh, H., Pippin, J., and Drebin, J. A. Down-regulation of HER2/*neu* expression induces apoptosis in human cancer cells that overexpress HER2/*neu*. *Cancer Res.*, *60*: 560–565, 2000.

37. Hsieh, S. S., Malerczyk, C., Aigner, A., and Czubyko, F. ErbB-2 expression is rate-limiting for epidermal growth factor-mediated stimulation of ovarian cancer cell proliferation. *Int. J. Cancer*, *86*: 644–651, 2000.

38. Bowman, T., Garcia, R., Turkson, J., and Jove, R. STATs in oncogenesis. *Oncogene*, *19*: 2474–2488, 2000.

39. Hynes, N. E., Horsch, K., Olayioye, M. A., and Badache, A. The ErbB receptor tyrosine family as signal integrators. *Endocrine-Related Cancer*, *8*: 151–159, 2001.

40. Olayioye, M. A., Neve, R. M., Lane, H. A., and Hynes, N. E. The ErbB signaling network: receptor heterodimerization in development and cancer. *EMBO J.*, *19*: 3159–3167, 2000.

41. Bera, T. K., Viner, J., Brinkmann, E., and Pastan, I. Pharmacokinetics and antitumor activity of a bivalent disulfide-stabilized Fv immunotoxin with improved antigen binding to erbB2. *Cancer Res.*, *59*: 4018–4022, 1999.